Acta Crystallographica Section D
Biological Crystallography
ISSN 0907-4449

Purification, crystallization and molecular symmetry of CDP-D-glucose 4,6-dehydratase from *Yersinia pseudotuberculosis*

Erik M. Vogan,[a]* Cornelia R. Bellamacina,[a] Xuemei He,[c] Bruce M. Foxman,[b] Dagmar Ringe,[a] Hung-Wen Liu[c] and Gregory A. Petsko[a]

[a]Department of Biochemistry, Rosenstiel Basic Medical Sciences Research Center, Brandeis University, Waltham, MA 02454, USA, [b]Department of Chemistry, Brandeis University, Waltham, MA 02454, USA, and [c]Division of Medicinal Chemistry, College of Pharmacy and Department of Chemistry and Biochemistry, University of Texas-Austin, Austin, TX 78712, USA

Correspondence e-mail: vogan@crystal.harvard.edu

Received 7 September 2001
Accepted 13 December 2001

The enzyme CDP-D-glucose 4,6-dehydratase (EC 4.2.1.45) is an NAD^+-dependent oxidoreductase which catalyzes the irreversible conversion of CDP-D-glucose to CDP-4-keto-6-deoxy-D-glucose. The product of this reaction is an intermediate in the synthesis of all CDP-linked 3,6-dideoxyhexoses, an important class of antigenic determinants found in the lipopolysaccharide layer of Gram-negative bacteria. Crystals of a recombinant form of this enzyme from *Yersinia pseudotuberculosis* have been grown in two crystal forms, both possessing pseudo-translational non-crystallographic symmetry, with dramatically different diffraction characteristics. A complete 1.8 Å data set has been collected from the primitive orthorhombic crystal form, for which the non-crystallographic symmetry is described in detail.

1. Introduction

The 3,6-dideoxyhexoses are important antigenic determinants, found primarily in the lipopolysaccharide layer of Gram-negative bacteria (Matsuhashi *et al.*, 1966; Samuelsson *et al.*, 1974; Makela & Stocker, 1984). In *Y. pseudotuberculosis*, the enzyme CDP-D-glucose 4,6-dehydratase (E_{od}) is responsible for the first committed step in the synthesis of all CDP-linked 3,6-dideoxyhexoses (Matsuhashi *et al.*, 1966; Samuelsson *et al.*, 1974). This enzyme is a dimer and requires NAD^+ cofactor, which is cycled fully during the course of the reaction (Matsuhashi *et al.*, 1966; Bevill, 1968; Glaser & Zarkowsky, 1971). When used in this fashion, the cofactor has been called a 'catalytic prosthetic group' and serves to define a small family of enzymes distinct from the larger family of NAD^+-utilizing enzymes, which carry out half-reactions (Walsh, 1979; Frey, 1996; He *et al.*, 1996). Unlike most members of this family, E_{od} requires exogenous NAD^+ for full activity (Matsuhashi *et al.*, 1964; Elbein & Heath, 1965; Yu *et al.*, 1992).

The irreversible biochemical reaction carried out by this enzyme has been studied extensively and is believed to proceed stepwise (Yu *et al.*, 1992) (Fig. 1). Firstly, a 4-keto intermediate is formed by cofactor-mediated oxidation, followed by dehydration and formation of a 5,6 double bond. This double bond is then reduced by enzyme-bound NADH (Bevill, 1968; Yu *et al.*, 1992). This mechanism is identical to that proposed for other nucleotide-linked 4,6-dehydratases (Snipes *et al.*, 1977; Walsh, 1979; Oths *et al.*, 1990). It is apparent from published studies that the dimeric enzyme has two cofactor-binding sites and that binding of cofactor to these two sites is anti-cooperative in nature (He *et al.*, 1996). Structures of several homologues have been solved, notably the dTDP-D-glucose 4,6-dehydratase from both *Salmonella enterica* serovar Typhimurium (Allard *et al.*, 2001; PDB code 1g1a) and *Escherichia coli* (Thoden *et al.*, 1999; PDB code 1bxk).

2. Experimental procedures

2.1. Bacterial expression and purification

All bacterial growth steps were performed at 310 K with shaking, while all purification steps were performed at 277 K, unless otherwise noted.

E. coli strain HB101, carrying plasmid pJT8 which encodes the *ascB* gene cloned from *Y. pseudotuberculosis*, was grown in 400 ml of Luria–Bertani broth supplemented with ampicillin at 100 μg ml^{-1} (Thorson *et al.*, 1994). This overnight culture was used at 100 ml l^{-1} to seed 2.8 l baffled growth flasks with 1 l of LB broth and 100 μg ml^{-1} ampicillin. These cultures grew for an additional 12 h prior to harvesting by centrifugation. Harvested cells were washed once with 120 ml purification buffer (100 m*M* potassium phosphate, 1 m*M* EDTA, pH 7.5), after which the cells were resuspended in 90 ml purification buffer and lysed by passing twice through a French press at 152 MPa chamber pressure. Cellular debris was removed by centrifugation at 35 000*g* for 45 min. The clarified crude supernatant was

Table 1
X-ray diffraction data.

Values in parentheses refer to the highest resolution shell.

X-ray source and wavelength	BNL NSLS X12B	BNL NSLS X12B
Space group	$P4_122$ or $P4_322$	$P2_12_12_1$
Unit-cell parameters (Å, °)	$a = b = 115.99$, $c = 255.54$, $\alpha = \beta = \gamma = 90.0$	$a = 99.90$, $b = 115.87$, $c = 126.83$, $\alpha = \beta = \gamma = 90.0$
Resolution range (Å)	84.50–3.80 (4.03–3.80)	36.30–1.80 (1.86–1.80)
No. of observations	166442	776823
No. of unique reflections	18123	133360
Mosaicity (°)	0.99	0.44
$I/\sigma(I)$	7.9 (5.2)	18.4 (2.6)
R_{sym} (%)	17.0 (31.8)	6.6 (35.0)
Completeness (%)	99.8 (99.8)	97.7 (93.4)

brought to 2%(*w*/*v*) streptomycin sulfate, stirred for 30 min and then centrifuged for 15 min at 13 300*g*. The supernatant was brought to 65% ammonium sulfate saturation and then stirred for 30 min, at which point E_{od} was precipitated by centrifugation at 13 300*g* for 20 min. The precipitate was resuspended in 20 ml ice-cold purification buffer and dialyzed against four 1 l changes of purification buffer. The dialysate was applied to a 340 ml Whatman DE-52 DEAE column equilibrated in purification buffer, then washed with 1.2 column volumes (cv) 3% buffer *B* (1.0 *M* potassium phosphate, 1 m*M* EDTA, pH 7.5), followed by a wash of 1.2 cv 4.5% buffer *B*. Partially purified E_{od} was then eluted with a linear gradient of 2.4 cv to 29.5% buffer *B*. Fractions were pooled based on OD_{280} measurements and 10% SDS–PAGE gels and then precipitated with 65% saturated ammonium sulfate. Precipitated protein was stored as a dry ammonium sulfate precipitate at 277 K. Immediately prior to the next chromatographic step, stored ammonium sulfate precipitate was resuspended in a minimal volume of ice-cold 50 m*M* potassium phosphate, 0.5 m*M* EDTA, pH 7.5. A 2 ml aliquot of resuspended protein was then run through a Pharmacia HiPrep 16/60 Sephacryl S-200 HR gel-filtration column equilibrated in the same buffer. Typically, five to eight gel-filtration runs were necessary to purify the entire sample. Pure enzyme eluted at a molecular weight of approximately 160 kDa, based on calibration of the column with Pharmacia LMW and HMW calibration kits. This is roughly the molecular weight expected of an enzyme tetramer. All peak fractions lacking significant contaminants, as demonstrated by 10% SDS–PAGE gels, were pooled and concentrated to 40 mg ml^{-1} (by Biorad dye-binding protein assay) using Amicon centriprep concentrators. Concentrated enzyme was flash-frozen in liquid nitrogen and stored at 193 K for later use. A typical enzyme preparation yielded approximately 100 mg of purified enzyme per litre of cell culture, with enzyme purity in excess of 95% as estimated by Coomassie Blue staining of a 10% SDS–PAGE gel.

2.2. Crystallization

Purified enzyme at 40 mg ml^{-1} was mixed in a 1:1 ratio with a solution of 5 m*M* CDP-D-glucose, 5 m*M* ADP-ribose and allowed to rest for 15 min at 277 K. Crystals were grown by the hanging-drop vapor-diffusion method at 298 K by mixing 5–10 µl of the enzyme/substrate/inhibitor solution with an equal volume of precipitant solution [1.0 *M* ammonium sulfate, 2%(*w*/*v*) Fluka PEG 4000, 100 m*M* Na MES pH 6.5, 0.001% thymol]. Needle-shaped crystals grew within a week to approximate dimensions of 0.4 × 0.15 × 0.15 mm (Fig. 2*a*). This crystal form exhibited 4/*m* symmetry when exposed to X-rays and will be called the tetragonal crystal form for the remainder of this report.

A second crystal form was generated by mixing purified enzyme at 40 mg ml^{-1} in a 1:1 ratio with 5 m*M* NAD^+ and allowing a 15 min rest at 277 K. The initial form II crystal was grown by the hanging-drop vapor-diffusion method at 298 K by mixing 10 µl of the enzyme/coenzyme solution with an equal volume of precipitant solution [1.0 *M* ammonium sulfate, 2%(*w*/*v*) Fluka PEG 4000, 100 m*M* K HEPES pH 7.5, 50 m*M* DTT]. This crystal took four weeks to appear and had approximate dimensions of 0.5 × 0.4 × 0.4 mm. All further crystals of this form were grown by the hanging-drop vapor-diffusion method at 277 K by mixing 4 µl of enzyme/coenzyme solution with an equal volume of precipitant solution minus DTT. After 2 d, these setups were micro-seeded with a 1 × 10^{-4} dilution of crushed form II crystals. Wedge- or box-shaped crystals grew within two weeks to approximate dimensions of 0.6 × 0.6 × 0.4 mm (Fig. 2*b*). This crystal form exhibited *mmm* symmetry when exposed to X-rays and will

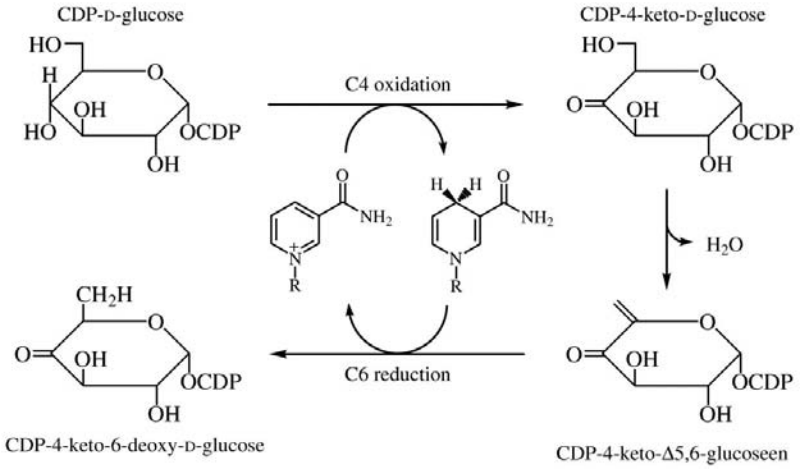

Figure 1
CDP-D-glucose 4,6-dehydratase reaction mechanism. Only the nicotinamide moiety of the NAD^+ cofactor has been shown.

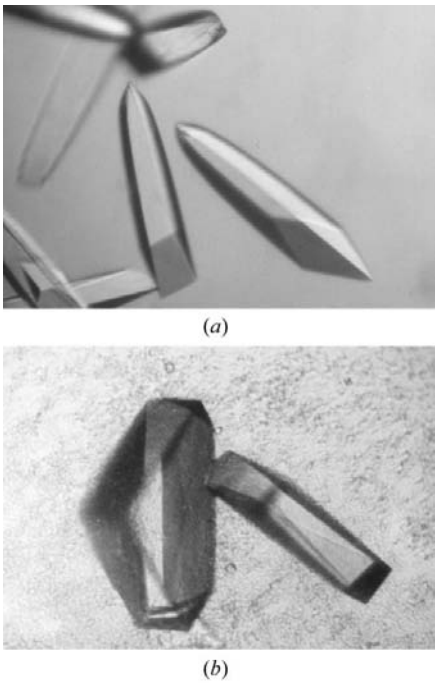

Figure 2
(*a*) Tetragonal crystal form. (*b*) Orthorhombic crystal form

be called the orthorhombic crystal form for the remainder of this report.

2.3. X-ray data collection and processing

Since both crystal forms were sensitive to temperature fluctuations of as little as 3 K, all crystals were frozen and all X-ray data collection was performed at 113 K. Tetragonal form crystals were passed briefly (<5 s) through cryoprotectant solution I [24% glycerol, 1.0 *M* ammonium sulfate, 2%(*w*/*v*) Fluka PEG 4000, 100 m*M* sodium MES pH 6.5 and 0.001% thymol] and then plunged into liquid nitrogen. Crystals processed in this way decayed at a much reduced rate, allowing the collection of a complete data set to 4.0 Å resolution at BNL NSLS synchrotron beamline X12B (Table 1). All data were reduced and scaled with the *HKL* suite of programs (Otwinowski & Minor, 1997; Gewirth, 1997). These crystals, identified as space group $P4_122$ (or the enantiomeric space group $P4_322$), had unit-cell parameters $a = b = 115.99$ Å, $c = 255.54$ Å with a pattern of systematically strong and weak reflections along the c^* reciprocal-lattice axis, indicative of approximate translational non-crystallographic symmetry. Assuming four enzyme monomers per asymmetric unit, the Matthews coefficient is 2.53 Å^3 Da^{-1} and the calculated solvent content is 51%, which are well within the accepted values.

Orthorhombic form crystals were passed stepwise between an artificial mother liquor [1.4 *M* ammonium sulfate, 2%(*w*/*v*) Fluka PEG 4000 and 100 m*M* K HEPES pH 7.5] and cryoprotectant solution II [1.4 *M* ammonium sulfate, 2%(*w*/*v*) Fluka PEG 4000, 25%(*w*/*v*) xylitol and 100 m*M* K HEPES pH 7.5], as noted in Table 2, and were then plunged into liquid nitrogen. A data set complete to 1.8 Å resolution was collected at BNL NSLS beamline X12B (Table 1). Again, all data were reduced and scaled with the *HKL* suite of programs (Otwinowski & Minor, 1997; Gewirth, 1997). These crystals, identified as space group $P2_12_12_1$, with unit-cell parameters $a = 99.90$, $b = 115.87$, $c = 126.83$ Å, showed a pattern of systematically weak reflections of class $2h + k = 4n + 2$, again indicative of approximate translational non-crystallographic symmetry. An assumption of four enzyme monomers per asymmetric unit leads to a calculated Matthews coefficient of 2.16 Å^3 Da^{-1} and 43% solvent content, which are well within the accepted values.

Table 2
Orthorhombic crystal form cryoprotection schedule.

Time (min)	[Xylitol] (%)
0	0.6
10	1.8
20	3.9
30	5.4
40	7.7
50	10.0
60	10.9
70	11.8
80	13.5
90	16.4
100	20.7
110	25.0

2.4. Non-crystallographic symmetry

The pattern of systematically weak reflections apparent along the c^* reciprocal-lattice axis of the tetragonal crystal form, reflected in the self-Patterson map shown in Fig. 3(*a*), indicates that a pseudo-translation of 0.472 relates two molecules along the *c* axis. Even given this initial relationship, it was not possible to model the remaining non-crystallographic symmetry operators for the tetragonal crystal form.

The orthorhombic crystal form shows a much more complex set of systematically weak reflections, which can be explained in terms of both the orthorhombic self-Patterson map (Fig. 3*b*) and the self-rotation map (Fig. 3*c*). The self-Patterson map indicates that a translation of approximately (0.5, 0.25, 0.0) relates at least two of the four enzyme monomers in the crystallographic asymmetric unit. The remaining relationships between the four monomers are obtained from the self-rotation map, which

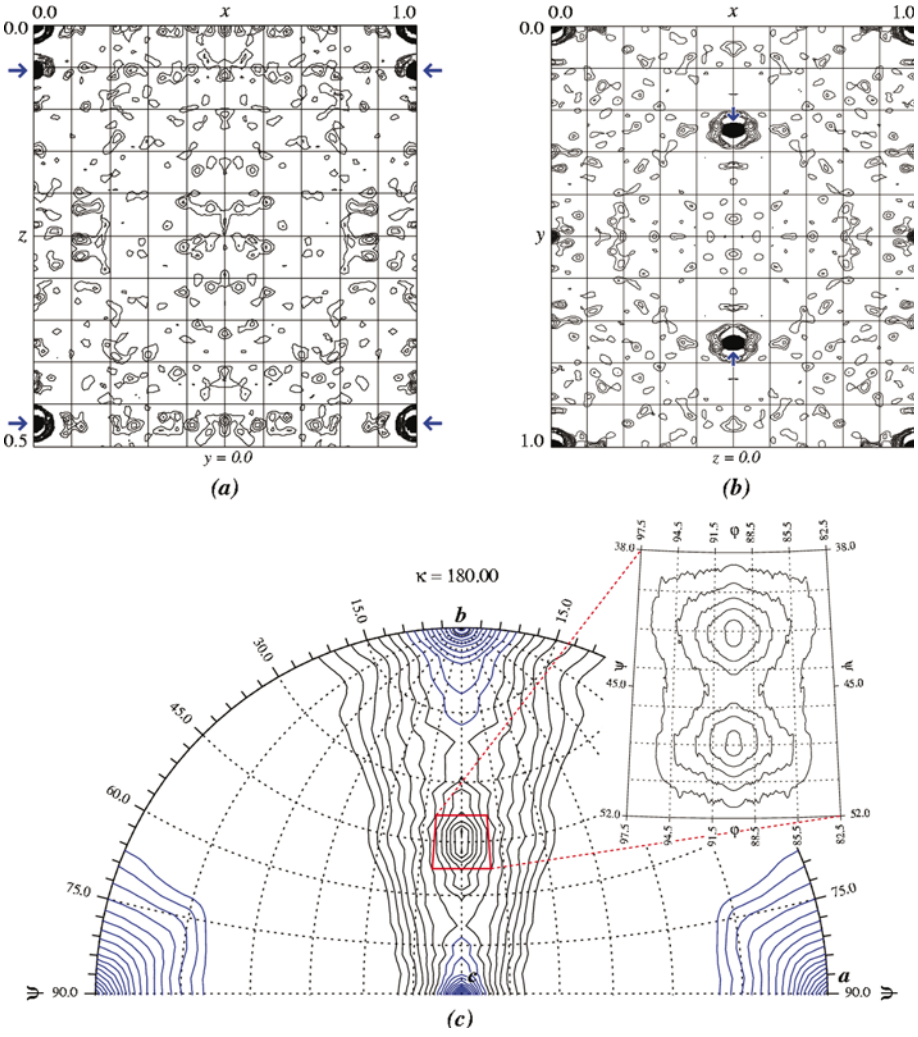

Figure 3
(*a*) Self-Patterson map of tetragonal form diffraction data, calculated using the *CCP*4 package (Collaborative Computational Project, Number 4, 1994). Map produced with the *XTALVIEW* package (McCree, 1993). (*b*) Self-Patterson map of orthorhombic form diffraction data. NCS-imposed pseudo-origin peaks have been marked with blue arrows. (*c*) Self-rotation map of orthorhombic form diffraction data, calculated using *GLRF* (Tong & Rossmann, 1997). Space-group imposed self-rotation peaks are blue. Inset shows twofold self-rotation peaks resulting from non-crystallography symmetry.

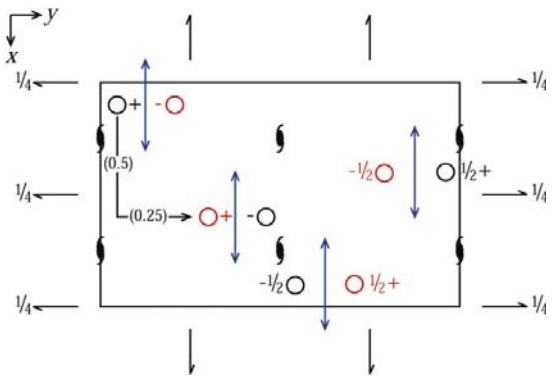

Figure 4
Packing and molecular symmetry model, showing interactions between the crystallographic and non-crystallographic symmetry elements. NCS twofold symmetry elements are in blue, while NCS-generated symmetry molecules are red.

shows two 90° rotations (inset, Fig. 3*c*) relating pairs of monomers. Given the placement of these 90° rotations on the *bc* axis of the rotation map, a third 90° rotation, leading to 222 symmetry, can be inferred parallel to the *a* axis, obscured in the self-rotation map by the crystallographic 2_1 screw axis. The packing and molecular symmetry model, shown in Fig. 4, was then built using these constraints. As can be seen, the twofold rotation axis parallel to the *a* axis crystallographic 2_1 symmetry operator would generate a translation in agreement with the observed translation vector of (0.5, 0.25, 0.0). The *b* and *c* components of the translation vector serve to fix the *y* and *z* coordinates of the molecular center of symmetry at (*x*, 0.125, 0.0). The *x* coordinate is ambiguous in such a situation and must be determined by either heavy-atom position-based or phase-based methods. Following the generation of an EMP derivative and solution of that heavy-atom partial structure, the molecular center of 222 symmetry was refined to (0.006, 0.124, 0.002).

3. Results

3.1. Non-crystallographic symmetry

Using fourfold non-crystallographic symmetry averaging in combination with phases from four isomorphous heavy-atom derivatives, the orthorhombic form was successfully phased to 1.8 Å resolution using the *CCP*4 suite of programs (Collaborative Computational Project, Number 4, 1994). The maps were of sufficient quality to allow 324 of the 357 amino acids in the prototypical monomer to be modeled on the first pass, leading to an $R_{\rm cryst}$ of 0.347 ($R_{\rm free} = 0.370$) after simulated-annealing torsional dynamics and grouped *B*-factor refinement (Brunger *et al.*, 1998). This model is currently being refined and extended to cover the missing regions.

This study was supported by grants GM032415 (to GAP) and GM035906 (to HWL) from the National Institutes of Health. We gratefully acknowledge BNL NSLS, Brookhaven, NY for the provision of synchrotron radiation and Malcolm Capel for his assistance in the collection of this data on beamline X12B. We also gratefully acknowledge Michael Rossmann for his assistance in interpreting the self-rotation maps.

References

Allard, S. T. M., Giraud, M.-F., Whitfield, C., Graninger, M., Messner, P. & Naismith, J. H. (2001). *J. Mol. Biol.* **307**, 283–295.
Bevill, R. D. (1968). *Biochem. Biophys. Res. Commun.* **30**, 595–599.
Brunger, A. T., Adams, P. D., Clore, G. M., DeLano, W. L., Gros, P., Grosse-Kunstleve, R. W., Jiang, J.-S., Kuszewski, J., Nilges, M., Pannu, N. S., Read, R. J., Rice, L. M., Simonson, T. & Warren, G. L. (1998). *Acta Cryst.* D**54**, 905–921.
Collaborative Computation Project, Number 4 (1994). *Acta Cryst.* D**50**, 760–763.
Elbein, A. D. & Heath, E. C. (1965). *J. Biol. Chem.* **240**, 1926–1931.
Frey, P. A. (1996). *FASEB J.* **10**, 461–470.
Gewirth, D. (1997). *The HKL Manual*, 5th ed. http://www.hkl-xray.com/hkl/manual_online.pdf.
Glaser, L. & Zarkowsky, H. (1971). *The Enzymes*, 3rd ed., edited by P. D. Boyer, Vol. 5, pp. 465–480. New York: Academic Press.
He, X., Thorson, J. S & Liu, H.-W. (1996). *Biochemistry*, **35**, 4721–4731.
McCree, D. E. (1993). *Practical Protein Crystallography*. San Diego: Academic Press.
Makela, P. H. & Stocker, B. A. D. (1984). *Handbook of Endotoxin*, edited by E. Th. Rietschiel, Vol. 1, pp. 59–137. New York: Elsevier.
Matsuhashi, S., Matsuhashi, M., Brown, J. G. & Strominger, J. L. (1964). *Biochem. Biophys. Res. Commun.* **15**, 60–64.
Matsuhashi, S., Matsuhashi, M. & Strominger, J. L. (1966). *J. Biol. Chem.* **241**, 4267–4274.
Oths, P. J., Mayer, R. M. & Floss, H. G. (1990). *Carbohydr. Res.* **198**, 91–100.
Otwinowski, Z. & Minor, W. (1997). *Methods Enzymol.* **276**, 307–326.
Samuelsson, K., Lindberg, B. & Brubaker, R. R. (1974). *J. Bacteriol.* **117**, 1010–1016.
Snipes, C. E., Brillinger, G.-U., Sellers, L., Mascaro, L. & Floss, H. G. (1977). *J. Biol. Chem.* **252**, 8113–8117.
Thoden, J. B., Hegeman, A. D., Frey, P. A. & Holden, H. M. (1999). Personal communication.
Thorson, J. S., Lo, S. F., Ploux, O., He, X. & Liu, H.-W. (1994). *J. Bacteriol.* **176**, 5483–5493.
Tong, L. & Rossmann, M. G. (1997). *Methods Enzymol.* **276**, 594–611.
Walsh, C. (1979). *Enzymatic Reaction Mechanisms.* New York: W. H. Freeman & Co.
Yu, Y., Russell, R. N., Thorson, J. S., Liu, L.-D. & Liu, H.-W. (1992). *J. Biol. Chem.* **267**, 5868–5875.